

In vivo force-length and activation dynamics of two distal rat hindlimb muscles in relation to gait and grade

Carolyn M. Eng^{1,2}, Nicolai Konow^{1,3}, Chris Tijs¹, Natalie C. Holt^{1,4}, and Andrew A. Biewener¹.

¹Concord Field Station, Department of Organismic and Evolutionary Biology, Harvard University, Bedford, MA, USA

²Department of Mechanical Engineering & Materials Science, Yale University

³Department of Biology, University of Massachusetts, Lowell

⁴Department of Biology, Northern Arizona University

Keywords: muscle, electromyography, work, gastrocnemius, plantaris, rat

Summary statement: Similar to the patterns observed in larger animals, distal rat muscles favor economy and show limited fascicle strains across gaits and grades.

Abstract

Muscle function changes to meet the varying mechanical demands of locomotion across different gait and grade conditions. A muscle's work output is determined by time-varying patterns of neuromuscular activation, muscle force and muscle length change, but how these patterns change under different conditions in small animals is not well-defined. Here we report the first integrated *in vivo* force-length and activation patterns in rats, a commonly used small animal model, to evaluate the dynamics of two distal hindlimb muscles (medial gastrocnemius, MG and plantaris, PL) across a range of gait (walk, trot, and gallop) and grade (level versus incline) conditions. We use these data to explore how the pattern of force production, muscle activation and muscle length changes across conditions in a small quadrupedal mammal. As hypothesized, we found that the rat muscles show limited fascicle strains during active force generation in stance across gaits and grades, indicating that these distal rat muscles generate force economically but perform little work, similar to patterns observed in larger animals during level locomotion. Additionally, given differences in fiber type composition and variation in motor unit recruitment across the gait and grade conditions examined here for these muscles, the *in vivo* force-length behavior and neuromuscular activation data reported here can be used to validate improved two-element Hill-type muscle models.

Introduction

Skeletal muscles undergo time-varying force development in relation to neuromotor activation that affect patterns of muscle length change and work output to mediate limb and body movements across varying locomotor behaviors. Understanding how these patterns change with gait and grade conditions is important for interpreting how muscle function is modulated in relation to time-varying biomechanical demands and how this is influenced by muscle-tendon architecture.

Prior studies examining the *in vivo* dynamics of muscle function during terrestrial locomotion have generally focused on the distal limb muscles of larger quadrupedal mammals (McGuigan et al., 2009), bipedal birds (Roberts et al., 1997; Daley and Biewener, 2003; Gabaldón et al., 2004), hopping wallabies (Biewener et al., 1998; Biewener et al., 2004), and humans (Lichtwark and Wilson, 2006b; Lichtwark et al., 2007). These studies have shown significant tendon energy recovery and limited net fascicle strain and net muscle work being performed by distal hindlimb muscles during steady level locomotion. While there is some debate around the consequences of such a strain pattern (Holt et al., 2014a; Curtin et al., 2019), it is generally accepted to be an economical force generating strategy. The cost of force generation is thought to be reduced when muscles contract isometrically, or undergo brief stretch-shorten contraction cycles with limited net muscle fascicle shortening, because this allows a smaller volume of muscle to be activated to produce a given force (Roberts et al., 1998; Biewener and Roberts, 2000).

When animals move up an incline, changes in limb muscle work are required to increase the animal's potential energy. In running turkeys (Roberts et al., 1997), guinea fowl (Daley and Biewener, 2003), and humans (Lichtwark et al., 2007), distal muscles (e.g. lateral gastrocnemius, LG or medial gastrocnemius, MG) increase fascicle shortening with modest changes in force to increase net muscle work during incline gait. However, in hopping wallabies, the LG and plantaris (PL) muscles exhibit little change in fascicle shortening relative to active lengthening, such that the net fascicle strain and work performed by wallaby distal hindlimb muscles remains low during incline as well as level hopping (Biewener et al., 2004), with more proximal muscles of wallabies likely contributing to the increase in work required (McGowan et al., 2007). In trotting and galloping goats, changes in fascicle

shortening and muscle force both contribute to the modulation of work by distal muscle-tendon units across differing grades. However, as with wallabies, within the hindlimb the majority of work needed to meet the potential energy demands of moving the body of the goat are primarily achieved by proximal limb muscles (McGuigan et al., 2009).

In comparison to studies of medium to large cursorial animals, it remains unclear how small animals adjust muscle force and work to meet varying demands of locomotion. Small mammals have relatively stout and stiff tendons (Ker et al., 1988) and crouched gait (Biewener, 1990). Both traits would be expected to require greater changes in muscle fascicle length and larger variations in force and work with respect to locomotor gait and grade compared with larger animals. However, our understanding of differences in muscle mechanics with gait and grade as a function of animal size is limited by the lack of measurements of muscle force from smaller animals.

Our goal in this study is to evaluate the *in vivo* dynamics of two distal hindlimb muscles (medial gastrocnemius, MG and plantaris, PL) of the rat across a range of gait (walk, trot, and gallop) and grade (level versus incline) conditions. This work builds on prior studies of muscle fascicle strain and activation of proximal and distal rat hindlimb muscles (Gillis and Biewener, 2002; Hodson-Tole and Wakeling, 2010b). However, these earlier studies lacked direct measurement of force from individual muscles. We also examine how patterns of muscle activation and force output vary in relation to fascicle strain during level versus incline conditions. Specifically, we aim to test the hypothesis (H1) that rat distal hindlimb muscles will exhibit limited fascicle shortening strains (here referred to as force economy) during level steady locomotion as previously observed in goats, turkeys, guinea fowl, and wallabies (Roberts et al., 1997; Daley and Biewener, 2003; Biewener et al., 2004; McGuigan et al., 2009), even though rats are small and traditionally considered non-cursorial (Hildebrand, 1988). We also hypothesize (H2) that the rat MG and PL muscles will show evidence of increased work on the incline compared with level and while trotting and galloping compared with walking. Finally, we hypothesize (H3) that the rat MG and PL will increase net fascicle shortening strain, as opposed to force output, to increase positive muscle work during incline gait, as was previously observed for two proximal muscles of the rat hindlimb (Gillis and Biewener, 2001; Gillis and Biewener, 2002).

Another goal of our study is to characterize the *in vivo* dynamics of rat MG and PL muscle function across a range of locomotor behaviors to provide direct measures that can be used to validate Hill-type models of these muscles. Using *in situ* measurements of rat MG and PL force-velocity and force-length properties (Holt et al., 2014b), two-element (fast and slow) Hill-type muscle models can be developed and compared to a traditional one-element model (Lee et al., 2013). These comparisons will allow for evaluations of the accuracy of Hill-type models for predicting the *in vivo* force and work performance of the muscles reported here. Comparison of *in vivo* measurements with muscle model outputs may then be used to evaluate which features of the model most strongly influence and improve the accuracy of predicted *in vivo* behavior. Furthermore, we selected the rat MG and PL muscles for this study because they have the greatest range of muscle fiber types (Armstrong and Phelps, 1984; Delp and Duan, 1996; Eng et al., 2008), and exhibit the greatest variation in motor unit recruitment (slow versus fast) across gait conditions relative to other plantarflexors in the rat (Hodson-Tole and Wakeling, 2008a). Relying on this variation in future studies will allow us to investigate how patterns of motor recruitment vary across speed and gait in relation to predicted patterns of force and work, derived from one- versus two-element Hill-type muscle models (Wakeling et al., 2012; Lee et al., 2013).

Material and methods

Animals and training

Eight Sprague Dawley rats (*Rattus norvegicus*, body mass: 369 ± 87 g) were obtained from Charles River Laboratories (Wilmington, MA, USA) and trained to run on a small, custom-built motorized treadmill (10 cm wide x 60 cm long). Rats were encouraged to locomote at three different gaits/speeds (walk: ~ 0.25 ms⁻¹; trot: ~ 0.50 ms⁻¹; gallop: ~ 0.75 ms⁻¹), which corresponded to Froude numbers of 0.05 for a walk, 0.31 for trot, and 1.13 for gallop. The rubber treadmill belt was textured to prevent slipping. Animals were encouraged to locomote and maintain position on the treadmill by gently tapping or briefly gusting their hindquarters with compressed air. Animals were trained over a period of two to three weeks to move as steadily as possible at each speed and gait on a level, as well as an inclined surface (14°, 24%

grade). Despite training, the rats did exhibit speed variation within a trial compared with treadmill studies of more cursorial animals (e.g. goats, guinea fowl and turkeys). All procedures were carried out under the approval of the Harvard University Faculty of Arts and Sciences Institutional Animal Care and Use Committee, according to USDA guidelines.

Surgical procedures

Once trained, the animal was anesthetized (isoflurane gas to effect via a small mask, 1-2%) and the right hindlimb and pelvis of the animal shaved and prepped (betadine scrub) for sterile surgery. Under anesthesia, skin openings were made over the posterior skull and nape of the neck, the pelvis, and a 2-3 cm opening made along the lateral aspect of the shank proximal to the calcaneus. All muscle transducers were disinfected in Cetylcyde™ solution (Cetylite, Inc., Pennsauken, NJ, USA) and rinsed repeatedly in sterile water before implantation. The skin openings were used to pass two sets of silver wire (California Fine Wire, Grover Beach, CA, USA) electromyography (EMG) electrodes, two pairs of 1-mm sonomicrometry electrodes (Sonometrics, Inc., London, Ontario, Canada), and two custom-fabricated 'leaf-spring' tendon force transducers (each 1.7 mm wide x 6.5 mm long). Tendon force transducers were manufactured and applied to the tendon following the methods described to record *Xenopus leavis* plantaris longus muscle-tendon forces (Richards and Biewener, 2007). Briefly, the leaf-spring tendon transducers were constructed from the aluminum wall of a soda can (Fig. 1 inset). Two thin aluminum strips were glued together along their length using Duro super glue™ (Loctite Corp., Avon, OH, USA) cyanoacrylate adhesive, after which a small metal foil strain gauge (FLK-1-11, Tokyo Sokki Kenkyujo, Ltd., Tokyo, Japan) was bonded using cyanoacrylate adhesive to the concave surface of the curved leaf spring (Fig. 1 inset). Following this, 36-gauge lead wires were soldered to the strain gauge and insulated with epoxy. Two short lengths (~ 6 cm) of 4-0 silk suture (Ethicon, Inc., Somerville, NJ, USA) were also epoxied to the surface of either end of the transducer (for anchoring the convex surface of the transducer against the tendon). The entirety of the transducer was then coated with M-Coat A (polyurethane curing agent, Micromeritics, Inc., Raleigh, NC, USA) to seal and insulate the circuit, eliminate adverse tissue reaction, and minimize tendon chafing. The shallow curvature of the aluminum functions as a leaf spring to allow tensile muscle forces

transmitted via the muscle's tendon to be measured by the strain gauge as the leaf spring is deflected under the applied load.

The tendon transducers were first anchored to the free tendons of the medial gastrocnemius (MG) and plantaris (PL) muscles. In rats, these tendons can be separated with sufficient length from the tendons of the soleus and the lateral gastrocnemius (Fig. 1). After securing each tendon force transducer on the isolated MG and PL tendons, a pair of sonomicrometry transducers and one or two 0.1 mm bi-polar offset hook (0.5 bared tip with 1.5 mm spacing) silver EMG electrodes were implanted mid-belly, aligned with the fascicle axis of the PL and MG muscles (Fig. 1). Alignment of the sonomicrometry crystals with the muscle's fascicle axis was verified post-mortem. In all cases, misalignment of crystals was $< 5^\circ$, such that errors in fascicle strain were $< 1\%$ due to misalignment. Crystal pairs were implanted approximately 8-10 mm apart, spanning $\sim 80\text{-}90\%$ of each muscle's fascicle length.

As both the MG and PL are unipennate muscles (Table S1), the sonomicrometry crystals were implanted through opposing superficial and deep aponeurotic surfaces of each muscle. Crystal alignment was adjusted to maximize the strength of the receiving signal by monitoring signal quality on an oscilloscope during surgical implantation. Sonomicrometry crystal lead wires and EMG electrodes were sutured in place using 5-0 silk. All transducer leads were adjusted to provide slack before closing the skin incisions (3-0 Vicryl, Ethicon, Inc.). Finally, a custom-designed head supported connector (constructed using three epoxy insulated GM-6 micro-connectors, Microtech, Inc., Boothwyn, PA, USA) was anchored to the skull using a 1-mm stainless-steel screw (MX-080-4; Small Parts, Inc., Logansport, IN, USA), after exposing a $\sim 1 \times 1\text{-cm}$ area of the skull, lightly scraping the periosteum and drilling a small hole through the parietal bone lateral to its medial suture. The skin surrounding the connector was then sutured tight using 3-0 Vicryl and further anchored using Vetbond™ adhesive (3M, Inc., Maplewood, MN, USA). Analgesics (Flunixin meglumine, 2 mg/kg) were administered every 12 hours for the 48 hours following surgery. In later experiments, the connector was anchored to the skin, instead of the skull, at its exit over the animal's neck using 3-0 Vicryl.

In vivo recordings

After recovering from surgery (24 to 48 hours), the lead-wire connectors mounted on the rats were connected to a shielded recording cable suspended by the

walls of the treadmill enclosure that transmitted sonomicrometry signals separately from the EMG and tendon-force transducers to recording amplifiers (EMG: Grass P-511, West Warwick, RI, USA, band-passed filtered 10-3000 Hz; sonomicrometry: Triton 120.2, Triton Technology Inc., San Diego, CA, USA, or Sonometrics, Inc., London, Ontario, Canada, and tendon force: Vishay 2120 bridge amplifier, Micromeritics, Raleigh, NC, USA). Sonomicrometry, EMG, and force transducer signals were sampled at 5 kHz in Acqknowledge™ software using a BioPac MP150 16-bit A/D converter (Biopac Systems, Inc., Goleta, CA, USA). Recordings were obtained while animals moved at a relatively steady speed within each gait at level or incline conditions.

Animals were also simultaneously recorded from a lateral view at 100 (walk) or 250 (trot and gallop) Hz using a Photron FastCam 1024 PCI video-camera (Photron Ltd, San Diego, CA, USA). Video recordings were post-triggered with a synchronization pulse transmitted to the muscle transducer A/D recordings. Video was used to determine the beginning of stance and swing phases using the time of touchdown and toe-off, respectively.

Following completion of the *in vivo* experimental recordings, the animals were euthanized using an intraperitoneal injection of an overdose of pentobarbital sodium. The MG and PL muscles and tendons were then isolated from the limb proximally at the knee joint with their attachments to the calcaneus and foot kept intact. The distal portion of each muscle (distal to the muscle transducer implants) was then cut, keeping its aponeurosis and tendon intact. The small portion of the distal muscle belly and aponeurosis was then anchored with 3-0 silk suture and frozen by submerging briefly in liquid nitrogen to anchor the suture tie. After assuring that the tendon transducer and tendon were warmed above room temperature (+22 °C), the frozen muscle end was then attached by the suture to a Kistler load cell (Model 9203, Amherst, NY, USA) and a series of tensile forces applied to the tendon with the foot held in place. This provided dynamic calibration coefficients of transducer strain gauge voltage output versus force recorded from the load cell. Calibrations (N/volt) were determined by regressing applied force against transducer voltage during the rise and fall in applied force. Regressions of the leaf-spring transducers yielded linear force-voltage profiles with $R^2 > 0.95$.

After calibrating the tendon force transducers, each sonomicrometry crystal pair was dissected free of its muscle attachment. The muscle belly was then sectioned

with a scalpel along a plane parallel to the fascicles to determine the locations of the sonomicrometry crystals with respect to the fascicle axis, allowing measurements of resting fascicle length and pennation angle to be determined. Muscle mass (M) and free tendon mass and length were then measured and recorded after being dissected free from the limb and foot. Muscle architecture measurements were made from dissected muscles for MG and PL in 5 of the 8 rats. Measurements of fascicle length (L_f) and pennation angle (θ) were measured and physiological cross-sectional area (PCSA) was calculated as:

$$PCSA = \frac{M \cdot \cos \theta}{\rho \cdot L_f}$$

where ρ is muscle density (1.056 g/cm³; Mendez and Keys, 1960). Normalization to mass or fiber length in the remaining rats, whose architecture was not measured, was performed using the average PL or MG mass and fiber length.

Data analysis

Force transducer, sonomicrometry, and EMG data were analyzed using a custom program written in Matlab (Mathworks, Natick, MA, USA) that is available upon request. The voltage signal from the sonomicrometry crystals was converted to millimeters using the Triton or Sonometrics sonomicrometers. Following Biewener et al. (1998) and Daley and Biewener (2003), length measures were multiplied by 1.0267 to account for the speed of sound in muscle (Goldman and Hueter, 1956; Hatta et al., 1988) and then an offset of 0.16 mm was applied to correct for the underestimate of length introduced by the crystal epoxy in the 1-mm crystal compared to the muscle. The calibrated sonomicrometry length signal was smoothed using a cubic smoothing spline with a spline tolerance of 0.00009 to interpolate dropouts in the signal caused by the receiving crystal briefly triggering off the wrong peak when there is a low signal-to-noise ratio at long fascicle lengths. The sonomicrometry signal was then low-pass filtered with a cutoff frequency of 15 Hz, which was $\sim 3x$ greater than the maximum stride frequency for a gallop. Following Roberts et al. (2007), the fascicle reference lengths for each animal were determined as the average lengths recorded during the entire stride cycle of a level trot. Ahn et al. (2018) show that operating range of the rat MG distal fascicles is evenly distributed about the plateau of their length-tension curve during trotting, indicating

that this method is a good estimate of resting length. Fascicle strains were calculated as sonomicrometry length changes normalized to fascicle reference length.

Tendon force signals were calibrated and filtered using a low-pass filter with a cutoff frequency of 5-15 Hz and then corrected to zero baseline. The cut-off frequency used for each gait was ~ 3x the average stride frequency with 5 Hz used for walking trials, 10 Hz for trotting, and 15 Hz for galloping. MG or PL stress was calculated as force divided by the individual's MG or PL PCSA. Peak MG and PL stress was calculated as the maximum MG and PL stress measured for each stride.

EMG recordings were filtered (60 Hz notch and 100-499 bandpass) before sampling. MG and PL EMG intensity were calculated as the average amplitude of the rectified signal within each stride and reported as a fraction of the maximum average amplitude recorded for each muscle within each individual (relative EMG intensity).

For each stride, the period of force production for each muscle was determined as the time between force rise and fall when force was above 10% of peak force. Positive and negative MG and PL fascicle strains were calculated as the sum of lengthening and shortening strains, respectively, measured during the period of force production in each stride. Net fascicle strains were calculated as the sums of positive and negative strains. MG and PL power were calculated as the product of muscle fascicle velocity and muscle force. Positive and negative MG and PL work were calculated as the integral of positive and negative power, respectively, summed over the period of force production. Net work was calculated as the sum of negative and positive work within each stride. Mass-specific work was calculated by normalizing muscle work values by muscle mass. Stride-based variables were averaged across two to four steady strides for each grade and gait trial within each individual. Across all trials for all conditions (gait x grade combinations) in all rats, there were two trials where only one steady stride was analyzed. Because of the challenging nature of the experiments and issues with implanted transducers and animal performance post-surgery (see discussion for details), data from a limited number of animals (as few as one in the case of PL work for incline walk) were obtained for some gait x grade conditions.

Statistical analyses

To analyze across gaits and grades, a general linear mixed model fit by maximum likelihood was implemented using R statistical software (v3.3.1; The R Foundation for Statistical Computing, Vienna, Austria). The model included gait and grade as fixed effects and individual as a random effect. A random effect of gait nested within individual was used if it significantly improved the model fit and the model had a lower AIC value. When the model fits a line for the effect of gait on a given response variable, the nested random effect allows the slope to vary among rats. An interaction term of grade and gait was also used if it significantly improved the model fit and the model had a lower AIC value. The non-parametric Wilcoxon signed-rank test was also used to compare differences between conditions because the small sample sizes often dictated that multiple variables violated the model assumptions and had non-normal distributions. In order to be consistent with previous *in vivo* studies, we report p-values obtained using the general linear mixed model in the results and in table 1, with the non-parametric p-values provided in table S3. Linear regression was used to evaluate the relationship between relative EMG intensity and peak stress. Data are reported as median (IQR) and p-values ≤ 0.05 were considered statistically significant.

Results

Individual patterns of MG and PL strain and force

Individual recordings of fascicle strain, force and EMG during level locomotion are shown for the MG (Fig. 2) and PL (Fig. 3) muscles. Three strides within each gait are shown. Both muscles are activated at or just prior to the onset of stance. In this individual, MG force develops and peaks just prior to mid-stance and decays to near zero just prior to or at the end of stance. Length and force patterns of the PL generally parallel those of the MG across gaits, although PL force peaks slightly later than the MG in this individual, at or after mid-stance (Fig. 3). As both muscles develop force, their fascicles initially continue to shorten from being passively

shortened during the end of swing. At faster gaits (particularly during galloping), final shortening of the MG and PL fascicles through the transition from stance to swing indicates passive shortening, associated with rapid ankle plantarflexion late in stance, prior to being dorsiflexed over the first half of swing. In MG, passive stretch of the fascicles, coincident with ankle dorsiflexion during swing is also evidenced by a brief peak in swing phase muscle force. Data for an additional individual for each muscle are shown in supplementary figure 1.

Muscle activation and peak muscle stress across gait and grade conditions

Across individuals, MG and PL motor recruitment, indicated by relative EMG intensity, increased with speed and change of gait for gallop compared with walk and trot (Fig. 4A,B). P-values obtained from the general linear mixed model are shown in Table 1 and reported here. Generally, similar patterns of recruitment for level (light gray) and incline (dark gray) conditions with changes in gait were observed for both muscles. However, whereas relative EMG intensity for MG was greater during incline versus level conditions for trot ($p=0.01$) and gallop ($p=0.02$), no significant change in relative EMG was observed for MG walk. PL relative EMG intensity was lower during incline gait for walk ($p=0.01$) and gallop ($p=0.04$) but not trot ($p=0.28$). In both MG and PL, relative EMG intensity was greater during gallop compared with walk (MG: $p<0.01$; PL: $p=0.01$) and gallop compared with trot (MG: $p=0.04$; PL: $p=0.05$). There was no significant change in EMG intensity from walk to trot (MG: $p=0.21$; PL: $p=0.46$).

Patterns of peak muscle stress (Fig. 4C,D) generally paralleled the patterns of relative EMG intensity measured across gait and grade conditions (Fig. S2), although differences were generally not significant. MG peak stress was significantly greater during incline compared with level walking ($p=0.04$). In PL, peak stress was significantly increased during galloping compared with walking ($p=0.01$).

Muscle fascicle strain patterns across gait and grade conditions

Changes in MG and PL fascicle strain, measured during active force generation during stance, showed generally consistent patterns for the two muscles across gait (Fig. 5); although some variation was observed in active shortening versus lengthening strain (and thus, net strain) across level versus incline gait conditions. No significant differences in MG lengthening or shortening strains were observed

across gaits or between incline and level. Across individuals, MG fascicles exhibited greater shortening than lengthening during stance (Fig. 5A), with the muscle undergoing net shortening over the course of stance in all conditions. MG net fascicle strain did not significantly vary with gait, ranging from -2.7% (interquartile range: -5.5 to -0.0%) for level galloping to -4.9% (IQR: -15.7 to -1.7%) for incline galloping. MG net strain significantly decreased on the incline compared with level for trot ($p=0.02$) and gallop ($p<0.01$). During level locomotion, shortening strains of MG fascicles were generally low, varying from -4.6% (IQR: -7.9 to -3.7%) for level trotting to -5.5% (IQR: -8.8 to -3.4%) for level galloping.

Active PL fascicles also generally shortened more than being actively stretched during force development, resulting in net PL shortening (Fig. 5B). However, no significant differences in PL lengthening or shortening strain occurred with gait, and PL shortening strain only decreased significantly during incline compared with level trot ($p<0.01$). Similar to MG, net PL fascicle strains were low, ranging from -1.3% (IQR: -6.6 to 1.5%) for level walking to -7.0% (IQR: -11.6 to -2.7%) for incline trotting across gait and grade conditions. As with the MG, PL fascicles also exhibited increased net shortening on the incline compared with level during trotting ($p<0.01$). During level locomotion, PL fascicle shortening strains were limited but higher than MG, ranging from -8.5% (IQR: -11.4 to -4.4%) for level trotting to -11.0% (IQR: -19.4 to -7.7%) for level walking.

Patterns of mass-specific muscle work across gait and grade conditions

Changes in MG and PL fascicle strain relative to force generation, resulted in mass-specific work loops (time-varying stress versus fascicle strain, Figs. 6 & 7) that exhibited positive work early and late in stance, with negative work or isometric force development in mid-stance. Muscle work patterns across rats were variable with the muscles of some rats producing net positive work, while others produced net negative work, as demonstrated by the two individuals for MG (Fig. 6) and PL (Fig. 7). This variability is also evidenced by the work loops shown for multiple individuals (Fig. S3) and the large group-level coefficients of variation for net muscle work (Table S2). Aside from the PL of rat 6 (Fig. 7), the MG and PL of the other rats exhibited little increase in net work output with a change from level to incline locomotion across all three gaits.

The average patterns of mass-specific work demonstrate that although there was substantial variation in negative versus positive mass-specific work across gait and grade conditions (Fig. 8), the net mass-specific work performed by the MG and PL was consistently low, averaging from -0.6 J kg^{-1} (interquartile range: -1.1 to 0.6 J kg^{-1}) for level walk to 1.9 J kg^{-1} (IQR: 0.4 to 3.1 J kg^{-1}) for incline trot in the MG and from -0.1 J kg^{-1} (IQR: -0.6 to 1.4 J kg^{-1}) for level trot to 3.4 J kg^{-1} (IQR: -1.5 to 11.0 J kg^{-1}) for incline gallop in the PL. Net work significantly increased on the incline compared with level for the MG during walking ($p=0.05$) and galloping ($p=0.01$). For the PL, net work also significantly increased on the incline compared with level for trotting ($p=0.01$) and galloping ($p=0.02$). The increase in net work was in part due to the increased positive work on the incline compared with level for PL trot ($p=0.02$) and gallop ($p=0.04$) and MG trot ($p=0.03$) and gallop ($p<0.01$). The increased PL net work during incline versus level trot was influenced by the significantly decreased negative work on the incline versus level ($p=0.04$).

There were few significant findings when comparisons were made using non-parametric statistics (Table S3). With these tests, there was significantly greater positive, negative, and net work for MG level trot compared with level walk and significantly greater MG EMG intensity for level gallop compared with level walk. Also, MG peak stress was significantly greater for level trot compared with level walk. To compare with previous *in vivo* studies, analysis from parametric statistics are referenced in the discussion.

Discussion

We report here the first integrated *in vivo* force-length and activation patterns of rat distal hindlimb muscles (medial gastrocnemius, MG and plantaris, PL) across different gaits and for level versus incline locomotion conditions. These results expand on earlier studies of myoelectric activation and fascicle strain reported for these muscles by Hodson-Tole and Wakeling (JEB 2008 & 2010). These earlier studies of rat hindlimb muscles focused on recruitment patterns over the course of stance and swing phases in relation to overall changes in fascicle strain and strain rate. Here, we find generally similar patterns of fascicle strain and activation for changes in gait and level versus incline locomotion. In these studies (here and

Hodson-Tole & Wakeling, 2008 & 2010), relative EMG intensity increased with speed and change of gait (Fig. 4A). However, by integrating *in vivo* recordings of muscle-tendon force, we provide more in-depth analysis of fascicle strain in relation to muscle force development during stance, with the ability to relate patterns of muscle activation to muscle force and work output across gait and grade conditions. The results of the parametric statistical tests are discussed here, which is consistent with previous *in vivo* studies and allows comparison with them (Gillis and Biewener, 2002; Daley and Biewener, 2003; Gabaldón et al., 2004; Lichtwark and Wilson, 2006a; Roberts et al., 2007; Higham and Biewener, 2008; Hodson-Tole and Wakeling, 2008b; McGuigan et al., 2009; Hodson-Tole and Wakeling, 2010a; Farris and Sawicki, 2012).

In support of our first hypothesis that the rat MG and PL muscles would show limited fascicle shortening strains during level locomotion, despite rats having stiffer tendons (Ker et al., 1988) and a more crouched gait (Biewener, 1990), we found that MG is activated and contracts over limited ranges of fascicle strain during active generation of stance force. During level locomotion, MG fascicle shortening strains were <6% across gaits. Although PL fascicle shortening strains were higher (<11% across gaits), these shortening strains for the rat MG and PL are comparable to those reported in larger animals that generate force economically including turkey, guinea fowl, and goat (Table 2). The limited shortening strains of the rat MG and PL corresponded to low levels of muscle work across level and incline gait conditions. Although net work by both muscles increased with a change from level to incline gait, the increases were generally small (Fig. 8) and, again, exhibited considerable variability across individual rats (Table S2). In part, this variability reflects the generally low levels of mass-specific net work performed by these two rat muscles in comparison to certain other limb muscles that have been studied (discussed below).

Our second hypothesis argued that MG and PL would show increased work with both gait/speed and grade. In partial support of this hypothesis, MG and PL generally showed significantly increased positive work on the incline compared with level. This increase in positive work resulted in a significant increase in net work on the incline compared with level for most gaits in MG and PL. In contrast to the changes in muscle work with grade, changes in gait/speed did not result in significant changes in positive or negative work for either muscle.

Consistent with our third hypothesis that increased work would occur through increased net shortening strain, we found net shortening strains significantly increased from level to incline locomotion for certain gaits (MG: trot and gallop; PL trot), as would be expected if the muscles contributed to the increased potential energy work requirement of incline gait. However, increased net shortening strain was not observed for either muscle during incline walking, or for the PL during incline galloping. In part, this reflects the variable nature of rat locomotion across successive strides, as well as among different individuals (Table S2), which limits statistical support for comparisons of certain muscle contractile patterns. Indeed, based on our non-parametric tests (Table S3), few of these differences were significant. In further support of hypothesis three, we found (based on either statistical approach) that peak MG and PL stress did not increase from level to incline locomotion for nearly all gait conditions.

The increase in relative EMG intensity and muscle force (or stress) with speed and gait observed in the rat MG and PL is also generally similar to that observed in the distal muscles of larger animals. Although changes in peak stress were generally not significant, MG and PL peak stress generally mirrored the changes in EMG intensity across conditions. Previous studies have found that increased EMG intensity (as a measure of the activated volume of a muscle) exhibits significant correlations with muscle force generation for a variety of muscles across gait and grade conditions (Daley and Biewener, 2003; Kaya et al., 2003; Roberts and Gabaldón, 2008b; McGuigan et al., 2009), as well as, in certain instances (Daley and Biewener, 2003), with net muscle work. Similarly, we found a significant relationship between relative EMG intensity and peak stress for both muscles across all gait conditions (Fig. S2; $p < 0.01$ for both muscles) with moderate R^2 of 58% for MG and 38% for PL. It appears that while PL and MG peak stresses mirrored increases in relative EMG intensity to some extent, the greater changes in EMG reflect increased motor recruitment required for the muscles to contract at higher strain rates when the rats locomote at higher speeds. EMG amplitude reflects the volume of active muscle but not the amplitude of muscle force because the amount of force that a volume of muscle produces depends on many factors, including muscle length, velocity, and activation/deactivation kinetics (Hof, 1984; Gabaldón et al., 2008; Roberts and Gabaldón, 2008a). When the muscle contracts at a higher rate, a greater volume of

muscle must be recruited to achieve the same level of force (Hof, 1984), which would explain increased EMG without concomitant increases in peak stress.

Variable patterns of rat MG and PL force-length and work output behavior

Although rat MG and PL muscles operated with limited net fascicle strains, both muscles underwent varying patterns of active shortening and lengthening. As a result, muscle work loops (Figs. 6 & 7) exhibited periods of positive and negative work at different phases of the support phase of the stride, including brief phases of limited strain during force generation, across locomotor conditions. Again, the stride to stride variability of the rats observed here within a gait, and across individuals, resulted in substantial variation in work loop behavior. The variability in muscle force-length behavior and resulting work output observed here for rats has generally not been observed in larger, more cursorial animals while running, trotting and hopping on motorized treadmills (Biewener et al., 1998; Daley and Biewener, 2003; Kaya et al., 2003; Gabaldón et al., 2004; McGuigan et al., 2009), for which coefficients of variation in muscle force and work output are much lower than those observed here for the rat MG and PL (Table S2).

Our rat experiments have a number of limitations resulting in the limited data and large variation seen here. Rat locomotion is inherently variable, with accelerations and decelerations occurring between consecutive steps even while the animal maintains an overall steady speed (Schmidt and Biknevicius, 2014), which likely contributes to the large inter-stride and inter-animal variability seen here. Furthermore, because of the competing demands post-surgery to allow the animals ample time to heal while minimizing post-surgery delay to ensure that the implanted transducers do not fail, limited data were obtained for some animals because of animal performance or transducer issues.

We acknowledge the issues regarding the use of parametric statistics with the limited and variable data reported here. Nevertheless, due to the challenging nature of *in vivo* muscle studies, such as this, past work assessing *in vivo* muscle function in relation to gait/speed and grade have relied on parametric statistics despite working with similarly small sample sizes and without reporting normality or variance (Gillis and Biewener, 2002; Daley and Biewener, 2003; Gabaldón et al., 2004; Lichtwark and Wilson, 2006a; Roberts et al., 2007; Higham and Biewener, 2008; Hodson-Tole and Wakeling, 2008b; McGuigan et al., 2009; Hodson-Tole and

Wakeling, 2010a; Farris and Sawicki, 2012). Consistent with these previous studies and to allow comparison with them, we used parametric statistics in our analysis but also included nonparametric analyses to provide a further more in-depth comparison (Table S3).

Rat distal hindlimb muscle force-length behavior in comparison to larger animals

Overall, there is some support for our first hypothesis that, although much smaller in size than bipedal and quadrupedal animals studied previously, having a more crouched gait, and traditionally considered a non-cursorial animal (Hildebrand, 1988), the rat MG exhibits limited fascicle strain to enhance force economy during level steady locomotion. Somewhat higher levels of shortening strains are seen in the PL muscle, but net PL fascicle strains are generally small and comparable to the MG. The lengthening, shortening and net fascicle strains recorded for rat MG and PL muscles fall within the ranges observed for the distal muscles of larger bipedal and quadrupedal animals that have been studied for level and incline conditions (Table 2), with the lowest strains observed for wallaby LG and PL muscles during steady level hopping (Biewener et al. 1998).

Although work output generally increased with incline gait, it remained low for both rat hindlimb muscles. The net mass-specific work performed by rat MG and PL muscles across level and incline conditions (ranging from 0.1 to 3.7 J kg⁻¹) also matched the relatively low levels observed in distal muscles of other larger species (Table 2), with net mass-specific work ranging from -0.8 to -5.0 J kg⁻¹ when distal muscles absorb energy, or from 0.1 to 8.3 J kg⁻¹ when producing energy across these larger species. The turkey peroneus longus and LG, guinea fowl LG, and goat LG and MG, show similar increases in net mass-specific work with grade but with generally higher magnitudes of net work in both the level and incline conditions (Daley and Biewener, 2003; Gabaldón et al., 2004; McGuigan et al., 2009).

The rat MG and PL muscles exhibited passive stretch and force development during swing (in response to ankle dorsiflexion) similar to that observed in the LG of running turkeys (Gabaldón et al., 2004; Nelson and Roberts, 2008). Passive force development during swing-phase stretch of the plantarflexors likely reflects activity of dorsiflexor antagonists to accelerate the foot in dorsiflexion. However, interestingly, passive force development during swing has not been observed in the turkey MG (Nelson and Roberts, 2008) or peroneus longus (Gabaldón et al., 2004), the guinea

fowl LG (Daley and Biewener, 2003), or the wallaby LG and PL muscles (Biewener et al., 1998); suggesting that the control of swing phase foot motion depends on the particular dynamics of muscle-tendon loading by the moving foot, as well as task-dependent specialization that may occur between muscle agonists (Nelson and Roberts, 2008).

Distal versus proximal muscle fascicle strain behavior across gait and grade conditions

The limited fascicle strains recorded *in vivo* during level locomotion in distal hindlimb muscles suggests that more proximal muscles may undergo greater fascicle strains (or varying force) to modulate limb work (Biewener and Daley, 2007), particularly when an animal moves over uneven terrain (e.g. producing work on inclines and recycling energy on the level), or when an animal accelerates or decelerates to change speed. However, challenges to measuring force in proximal muscles makes it difficult to demonstrate whether a proximo-distal gradient exists in relation to the role and architecture of limb muscles for modulating work versus generating force economically, as has been previously argued (Daley et al., 2007).

In comparison to the limited net fascicle strains we observe here for rat MG and PL muscles, more substantial net fascicle shortening or lengthening strains were observed during stance in proximal muscles of the rat hind limb. Recordings of *in vivo* fascicle strain of the rat biceps femoris (BF, a hip extensor and knee flexor) and vastus lateralis (VL, a knee extensor) showed that the BF actively shortens (-20 to -22%) and the VL is stretched whilst activated (10 to 16%) across level walk, trot and gallop gaits (Gillis and Biewener, 2001). Our third hypothesis that the rat MG and PL muscles would increase net fascicle shortening during incline gait, as previously observed for the more proximal BF and VL muscles (Gillis and Biewener, 2002), however, was only partially supported, as increased net fascicle shortening strain occurred in the MG during incline trotting and galloping but not during walking, and was only observed in the PL during incline trotting. Together, these data further suggest that proximal muscles play a more important role in modulating limb work across grades.

Use of in vivo recordings of muscle contractile function to validate muscle models

Despite the inherent variability of rat locomotion, our ability to obtain recordings

of rat MG and PL muscle force-length behavior in relation to neuromuscular activation (EMG) and work output across different gaits and grade conditions provides the opportunity to further explore the use of direct *in vivo* measures of contractile dynamics to validate Hill-type models based on these muscles. In-depth *in situ* measurements of MG and PL force-velocity and force-length properties (Holt et al., 2014b) will facilitate the development of improved two-element (fast and slow) Hill-type muscle models that can be compared to traditional one-element models. Recent efforts to develop more accurate two-element models based on *in situ* muscle measurements in goats (Lee et al., 2013) and humans (Dick et al., 2017) have had limited success for improving their accuracy to predict *in vivo* force and work performance compared with traditional one-element models. This is due, in part, to the limited quality of muscle contractile and architectural properties obtained for these muscles, as well as challenges in determining muscle slack length for the motor tasks that were studied. By incorporating higher quality contractile and architectural properties into models of rat muscles, model features that most strongly influence and improve the accuracy of predicted *in vivo* behavior can be better identified and achieved. The broad range of fiber types (Armstrong and Phelps, 1984; Delp and Duan, 1996; Eng et al., 2008) and variation in motor unit recruitment across gait conditions (Hodson-Tole and Wakeling, 2008a) for these distal rat muscles will also facilitate examination of how patterns of motor recruitment affect model dynamics of muscle function.

Acknowledgements

We are grateful for Pedro Ramirez for assistance with animal care. We thank Maria Miara and Ana Garcia for collecting pilot data for this work. We also appreciate the constructive feedback from three referees that improved the quality of the manuscript.

Competing Interests

No competing interests declared.

Author Contributions

Conceptualization: A.A.B., C.M.E., N.K.; Methodology: A.A.B., C.M.E., C.T., N.K.; Formal analysis: all authors; Investigation: all authors.; Resources: A.A.B., N.K.; Data curation: all authors; Writing - original draft: C.M.E., A.A.B.; Writing - review & editing: all authors; Supervision: A.A.B., N.K., Funding acquisition: A.A.B.

Funding

This work was supported by the National Institutes of Health [2R01AR055648 to A.A.B.].

References

- Ahn, A., Konow, N., Tijs, C. and Biewener, A.** (2018). Different segments within vertebrate muscles can operate on different regions of their force–length relationships. *Integr. Comp. Biol.* **58**, 219-231.
- Armstrong, R. B. and Phelps, R. O.** (1984). Muscle fibre type composition of the rat hindlimb. *Am. J. Anat.* **171**, 259–272.
- Biewener, A. A.** (1990). Biomechanics of mammalian terrestrial locomotion. *Science* **250**, 1097-1103.
- Biewener, A. A. and Daley, M. A.** (2007). Unsteady locomotion: integrating muscle function with whole body dynamics and neuromuscular control. *J. Exp. Biol.* **210**, 2949-2960.
- Biewener, A. A., Konieczynski, D. D. and Baudinette, R. V.** (1998). In vivo muscle force-length behavior during steady-speed hopping in tammar wallabies. *J. Exp. Biol.* **201**, 1681-1694.
- Biewener, A. A., McGowan, C. P., Card, G. M. and Baudinette, R. V.** (2004). Dynamics of leg muscle function in tammar wallabies (*M. eugenii*) during level versus incline hopping. *J. Exp. Biol.* **207**, 211-223.
- Biewener, A. A. and Roberts, T. J.** (2000). Muscle and tendon contributions to force, work, and elastic energy savings: a comparative perspective. *Exer. Sport Sci. Rev.* **28**, 99-107.
- Curtin, N. A., Woledge, R. C., West, T. G., Goodwin, D., Piercy, R. J. and Wilson, A. M.** (2019). Energy turnover in mammalian skeletal muscle in contractions mimicking locomotion: effects of stimulus pattern on work, impulse and energetic cost and efficiency. *J. Exp. Biol.*, jeb. 203877.
- Daley, M. A. and Biewener, A. A.** (2003). Muscle force-length dynamics during level *versus* incline locomotion: a comparison of *in vivo* performance of two guinea fowl ankle extensors. *J. Exp. Biol.* **206**, 2941-2958.
- Daley, M. A., Felix, G. and Biewener, A. A.** (2007). Running stability is enhanced by a proximo-distal gradient in joint neuromechanical control. *J. Exp. Biol.* **210**, 383-394.
- Delp, M. D. and Duan, C.** (1996). Composition and size of type I, IIA, IID/X and IIB fibres and citrate synthase activity of rat muscle. *J. Appl. Physiol.* **80**, 261–270.
- Dick, T. J. M., Biewener, A. A. and Wakeling, J. M.** (2017). Comparison of human gastrocnemius forces predicted by Hill-type muscle models and estimated from ultrasound images. *J. Exp. Biol.* **220**, 1643-1653.
- Eng, C. M., Smallwood, L. H., Rainiero, M. P., Lahey, M., Ward, S. R. and Lieber, R. L.** (2008). Scaling of muscle architecture and fiber types in the rat hindlimb. *J. Exp. Biol.* **211**, 2336-2345.
- Farris, D. J. and Sawicki, G. S.** (2012). Human medial gastrocnemius force–velocity behavior shifts with locomotion speed and gait. *Proc. Natl. Acad. Sci.* **109**, 977-982.

Gabaldón, A. M., Nelson, F. E. and Roberts, T. J. (2004). Mechanical function of two ankle extensors in wild turkeys: shifts from energy production to energy absorption during incline *versus* decline running. *J. Exp. Biol.* **207**, 2277-2288.

Gabaldón, A. M., Nelson, F. E. and Roberts, T. J. (2008). Relative shortening velocity in locomotor muscles: turkey ankle extensors operate at low V/V_{max} . *American Journal of Physiology-Regulatory, Integrative and Comparative Physiology* **294**, R200-R210.

Gillis, G. B. and Biewener, A. A. (2001). Hindlimb muscle function in relation to speed and gait: in vivo patterns of strain and activation in a hip and knee extensor of the rat (*Rattus norvegicus*). *J. Exp. Biol.* **204**, 2717-2731.

Gillis, G. B. and Biewener, A. A. (2002). Effects of surface grade on proximal hindlimb muscle strain and activation during rat locomotion. *J. Appl. Physiol.*

Goldman, D. E. and Hueter, T. F. (1956). Tabular data of the velocity and absorption of high-frequency sound in mammalian tissues. *The Journal of the Acoustical Society of America* **28**, 35-37.

Hatta, I., Sugi, H. and Tamura, Y. (1988). Stiffness changes in frog skeletal muscle during contraction recorded using ultrasonic waves. *J. Physiol* **403**, 193-209.

Higham, T. E. and Biewener, A. A. (2008). Integration within and between muscles during terrestrial locomotion: effects of incline and speed. *J. Exp. Biol.* **211**, 2303-2316.

Hildebrand, M. B. (1988). *Analysis of Vertebrate Structure*, 3rd. ed. New York: Wiley and Sons.

Hodson-Tole, E. F. and Wakeling, J. (2010a). The influence of strain and activation on the locomotor function of rat ankle extensor muscles. *J. Exp. Biol.* **213**, 318-330.

Hodson-Tole, E. F. and Wakeling, J. M. (2008a). Motor unit recruitment patterns 1: responses to changes in locomotor velocity and incline. *J. Exp. Biol.* **211**, 1882-1892.

Hodson-Tole, E. F. and Wakeling, J. M. (2008b). Motor unit recruitment patterns 2: the influence of myoelectric intensity and muscle fascicle strain rate. *J. Exp. Biol.* **211**, 1893-1902.

Hodson-Tole, E. F. and Wakeling, J. M. (2010b). The influence of strain and activation on the locomotor function of rat ankle extensor muscles. *J Exp Biol* **213**, 318-330.

Hof, A. L. (1984). EMG and muscle force: an introduction. *Human Movement Science* **3**, 119-153.

Holt, N. C., Roberts, T. J. and Askew, G. N. (2014a). The energetic benefits of tendon springs in running: is the reduction of muscle work important? *J Exp Biol* **217**, 4365-4371.

Holt, N. C., Wakeling, J. M. and Biewener, A. A. (2014b). The effect of fast and slow motor unit activation on whole-muscle mechanical performance: the size principle may not pose a mechanical paradox. *Proc. R. Soc. Lond. B. Biol. Sci.* **281**, 1-6.

Kaya, M., Leonard, T. and Herzog, W. (2003). Coordination of medial gastrocnemius and soleus forces during cat locomotion. *J. Exp. Biol.* **206**, 3645-3655.

Ker, R. F., Alexander, R. M. and Bennett, M. B. (1988). Why are mammalian tendons so thick? *J. Zool., Lond.* **216**, 309-324.

Lee, S. S. M., de Boef Miara, M., Arnold, A. S., Biewener, A. A. and Wakeling, J. M. (2013). Accuracy of gastrocnemius forces in walking and running goats predicted by one-element and two-element Hill-type models. *J. Biomech.* **43**, 2288-2295.

Lichtwark, G. and Wilson, A. (2006a). Interactions between the human gastrocnemius muscle and the Achilles tendon during incline, level and decline locomotion. *J. Exp. Biol.* **209**, 4379-4388.

Lichtwark, G. A., Bougoulias, K. and Wilson, A. M. (2007). Muscle fascicle and series elastic element length changes along the length of the human gastrocnemius during walking and running. *J. Biomech.* **40**, 157-164.

Lichtwark, G. A. and Wilson, A. M. (2006b). Interactions between the human gastrocnemius muscle and the Achilles tendon during incline, level and decline locomotion. *J. Exp. Biol.* **209**, 4379-4388.

McGowan, C. P., Baudinette, R. V. and Biewener, A. A. (2007). Modulation of proximal muscle function during level versus incline hopping in tammar wallabies (*Macropus eugenii*). *J. Exp. Biol.* **210**, 1255-1265.

McGuigan, M. P., Yoo, E., Lee, D. V. and Biewener, A. A. (2009). Dynamics of goat distal hind limb muscle-tendon function in response to locomotor grade. *J. Exp. Biol.* **212**, 2092-2104.

Mendez, J. and Keys, A. (1960). Density and composition of mammalian muscle. *Metabolism.* **9**, 184-188.

Nelson, F. E. and Roberts, T. J. (2008). Task-dependent force sharing between muscle synergists during locomotion in turkeys. *J. Exp. Biol.* **211**, 1211-1220.

Richards, C. T. and Biewener, A. A. (2007). Modulation of in vivo muscle power output during swimming in the African clawed frog (*Xenopus laevis*). *J. Exp. Biol.* **210**, 3147-3159.

Roberts, T. J., Chen, M. S. and Taylor, C. R. (1998). Energetics of bipedal running II. Limb design and running mechanics. *J. Exp. Biol.* **201**, 2753-2762.

Roberts, T. J. and Gabaldón, A. M. (2008a). Interpreting muscle function from EMG: lessons learned from direct measurements of muscle force. *Integr. Comp. Biol.* **48**, 312-320.

Roberts, T. J. and Gabaldón, A. M. (2008b). Interpreting muscle function from EMG: lessons learned from direct measurements of muscle force. *Int. Comp. Biol.* **48**, 312–320.

Roberts, T. J., Higginson, B. K., Nelson, F. E. and Gabaldón, A. M. (2007). Muscle strain is modulated more with running slope than speed in wild turkey knee and hip extensors. *J. Exp. Biol.* **210**, 2510-2517.

Roberts, T. J., Marsh, R. L., Weyand, P. G. and Taylor, C. R. (1997). Muscular force in running turkeys: the economy of minimizing work. *Science* **275**, 1113-1115.

Schmidt, A. and Biknevicius, A. R. (2014). Structured variability of steady-speed locomotion in rats. *J. Exp. Biol.* **217**, 1402-1406.

Wakeling, J. M., Lee, S. S. M., Arnold, A. S., de Boef Miara, M. and Biewener, A. A. (2012). A muscle's force depends on the recruitment patterns of its fibers. *Ann. Biomed. Eng.* **40**, 1708-1720.

Figures

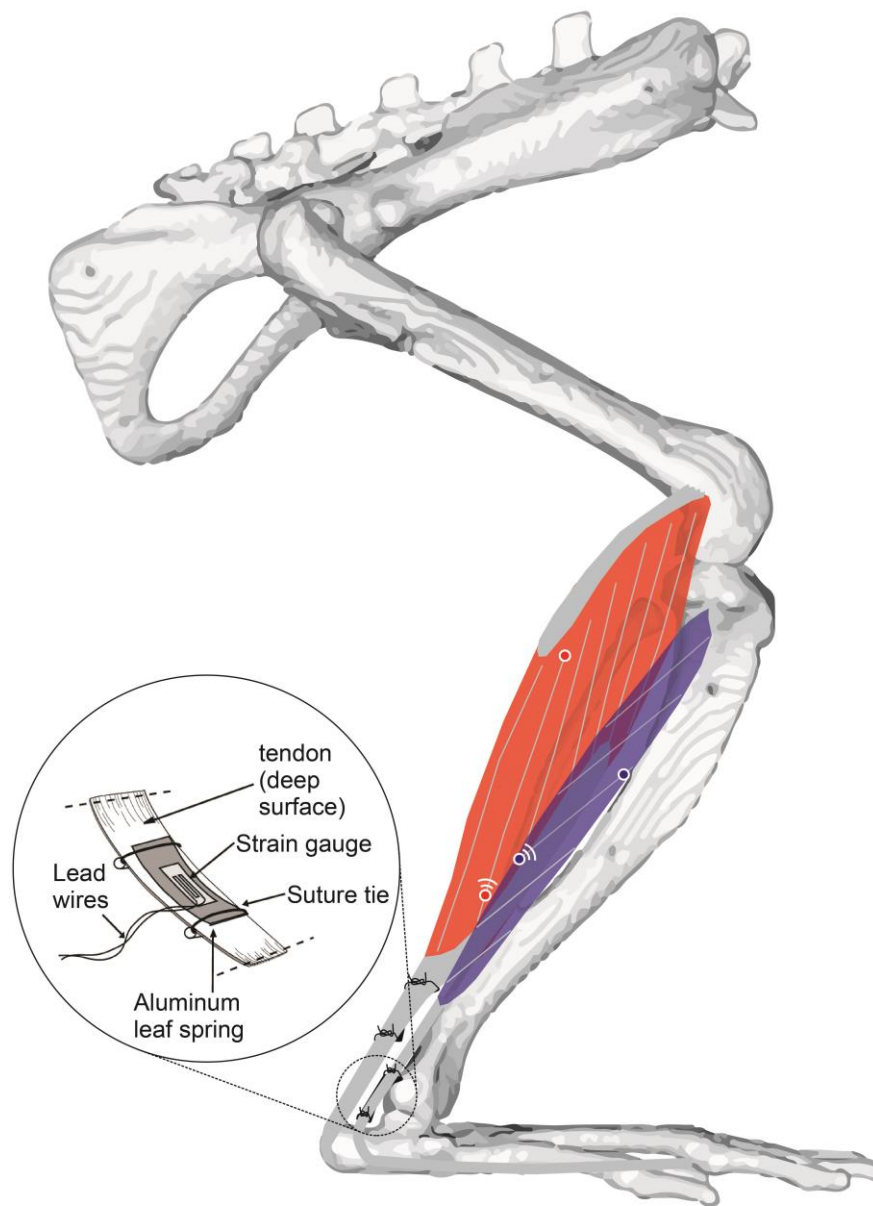


Figure 1. Sonomicrometry and EMG electrodes were implanted in the bellies of the plantaris (PL; blue) and medial gastrocnemius (MG; red) muscles, together with custom-designed 'leaf-spring' force transducers attached to each muscle's tendon using 4-0 silk sutures proximal to the calcaneus (see inset). The sonomicrometry crystals were implanted parallel to the fascicle axis of each muscle, with the EMG electrodes implanted in immediately adjacent regions.

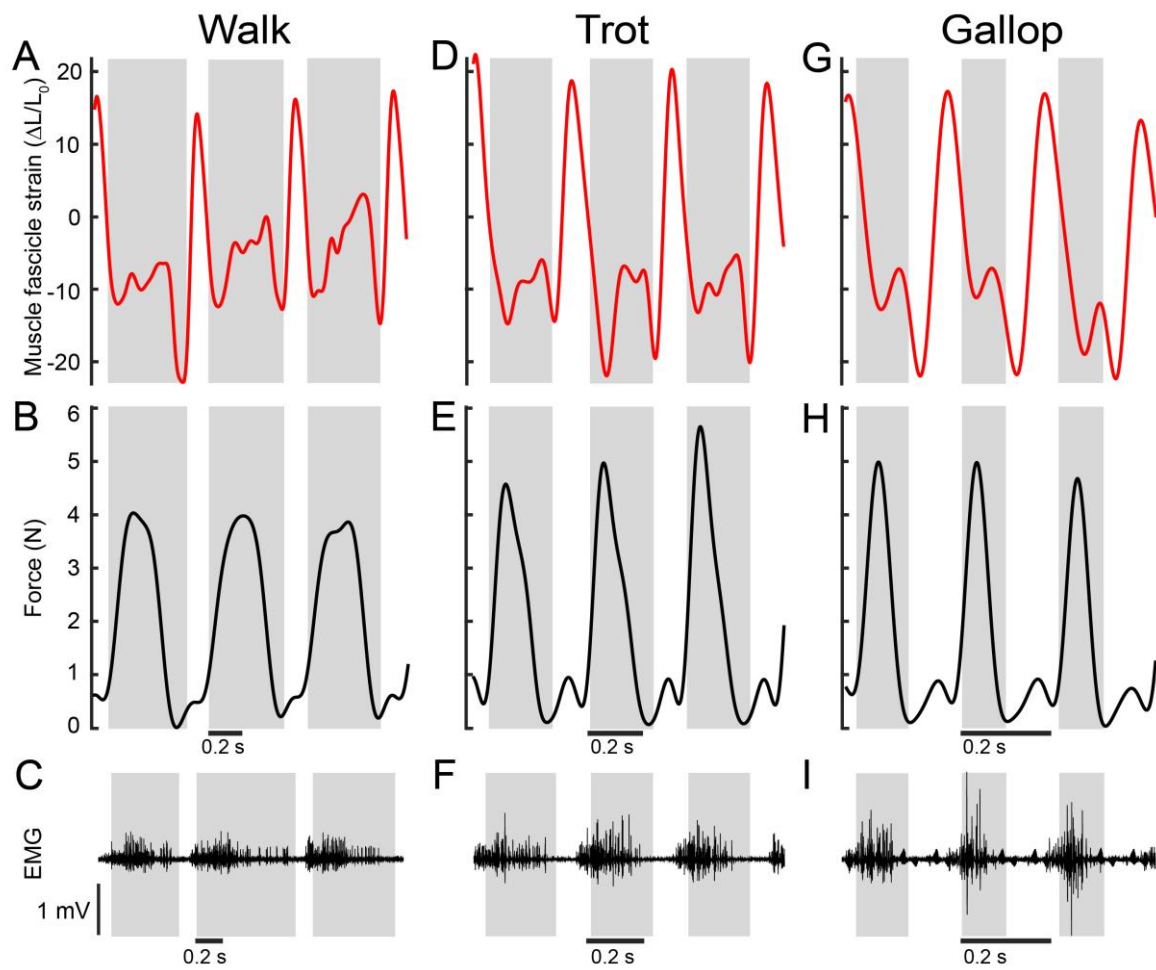


Figure 2. MG muscle fascicle strain (A, D, G), muscle force (B, E, H), and unamplified EMG (C, F, I) in one individual for a level walk, trot, and gallop. Gray regions represent the stance phase of each stride. Note that the time scale is expanded for the faster speeds and gaits. For walk and trot, the same rat was used for muscle fascicle strain and force, while a different rat was used for EMG measurements.

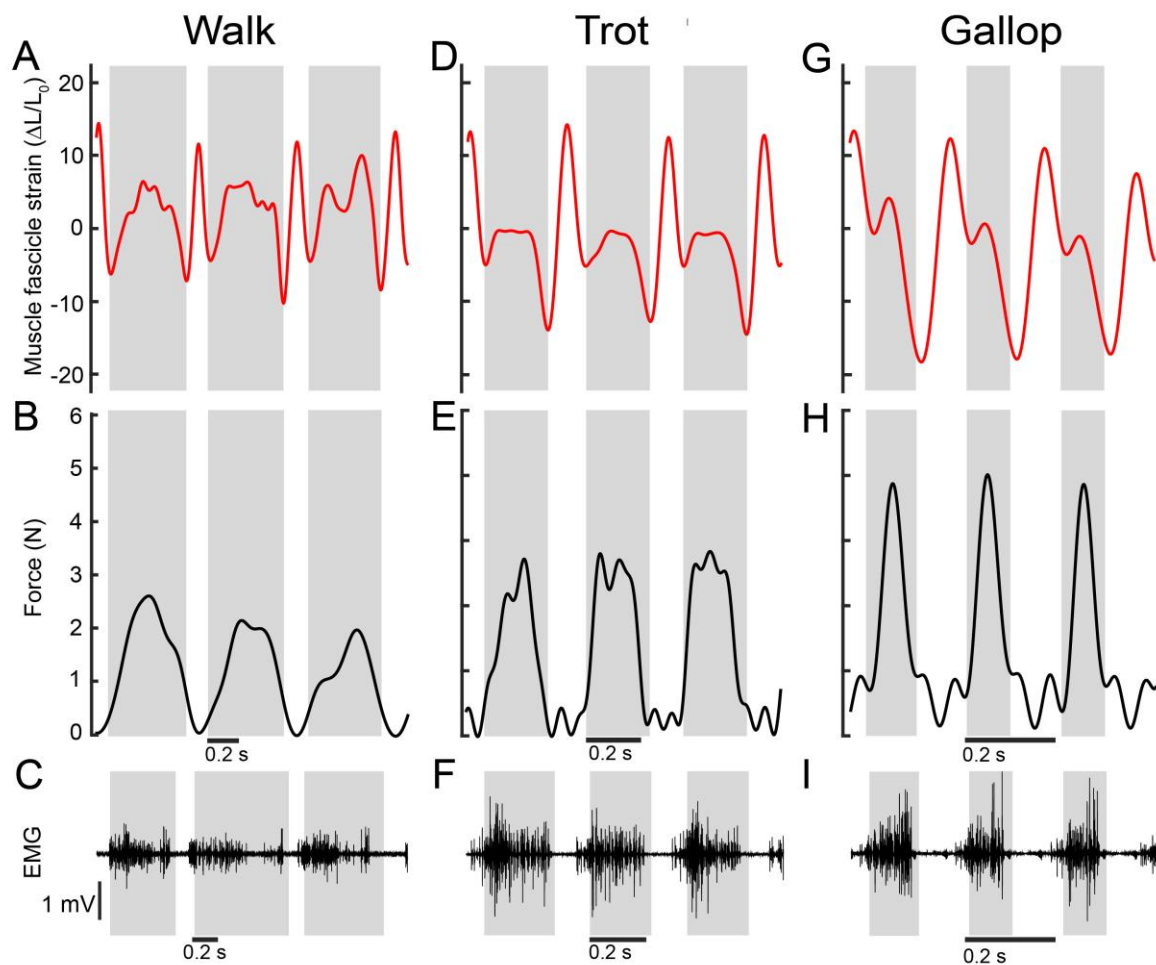


Figure 3. PL muscle fascicle strain (A, D, G), muscle force (B, E, H), and unamplified EMG (C, F, I) in one individual for level walk, trot, and gallop. Gray regions represent the stance phase of each stride. Note that the time scale is expanded for the faster speeds and gaits. For walk and trot, the same rat was used for muscle fascicle strain and force, while a different rat was used for EMG measurements.

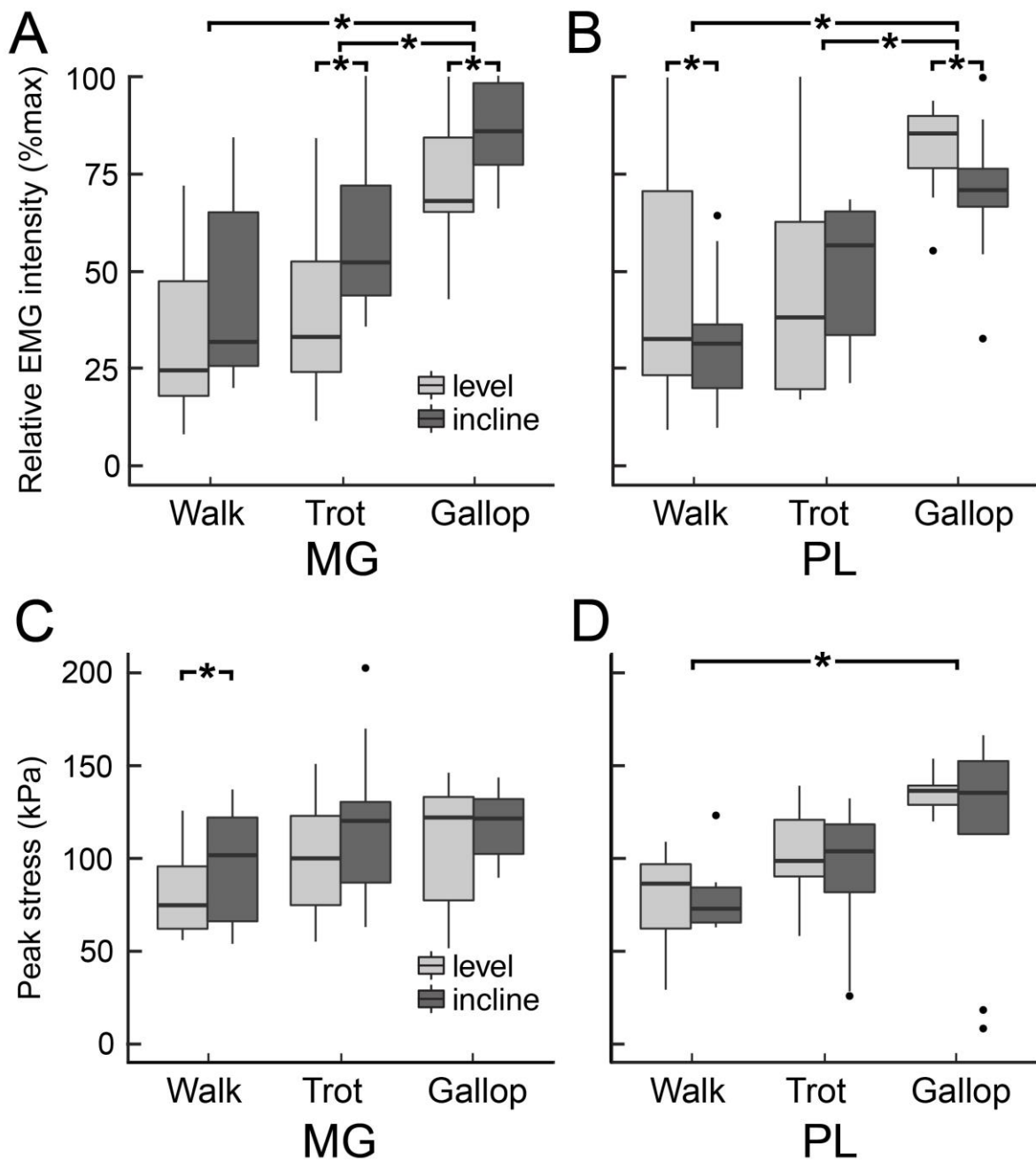


Figure 4. Boxplots showing relative EMG intensity in rat MG (A) and PL (B) and peak stress in rat MG (C) and PL (D) for walk, trot, and gallop on level (light gray) versus incline (dark gray). The EMG data demonstrates increased motor recruitment in the gallop compared with walk and trot in both muscles. MG (A) exhibits increased motor recruitment on the incline versus level for trot and gallop. In contrast, PL (B) exhibits increased recruitment on level versus incline for walk and gallop. Peak stress is greater on the incline versus level walk in the MG (C) and peak stress is greater during galloping compared with walking in the PL muscle (D). Data reported as median with the bars extending to the first and third quartiles and whiskers showing the minimum and maximum values excluding outliers (greater than $1.5 \times IQR$), which are shown as single data points. Statistically significant differences

are indicated with an asterisk ($p < 0.05$) as evaluated using a general linear mixed model. For EMG, N=6 for MG level walk, MG incline trot, PL level walk, PL level trot; N=5 for MG incline walk, MG level trot, MG level gallop, PL incline walk, PL incline trot; and N=4 for MG incline gallop, PL incline gallop, N=3 for PL level gallop. For peak stress, N=6 for MG level walk, MG level trot; N=5 for PL level walk, PL level trot, MG incline trot; N=4 for MG incline walk, MG level gallop, MG incline gallop, PL incline trot, PL incline gallop; and N=2 for PL incline walk and PL level gallop.

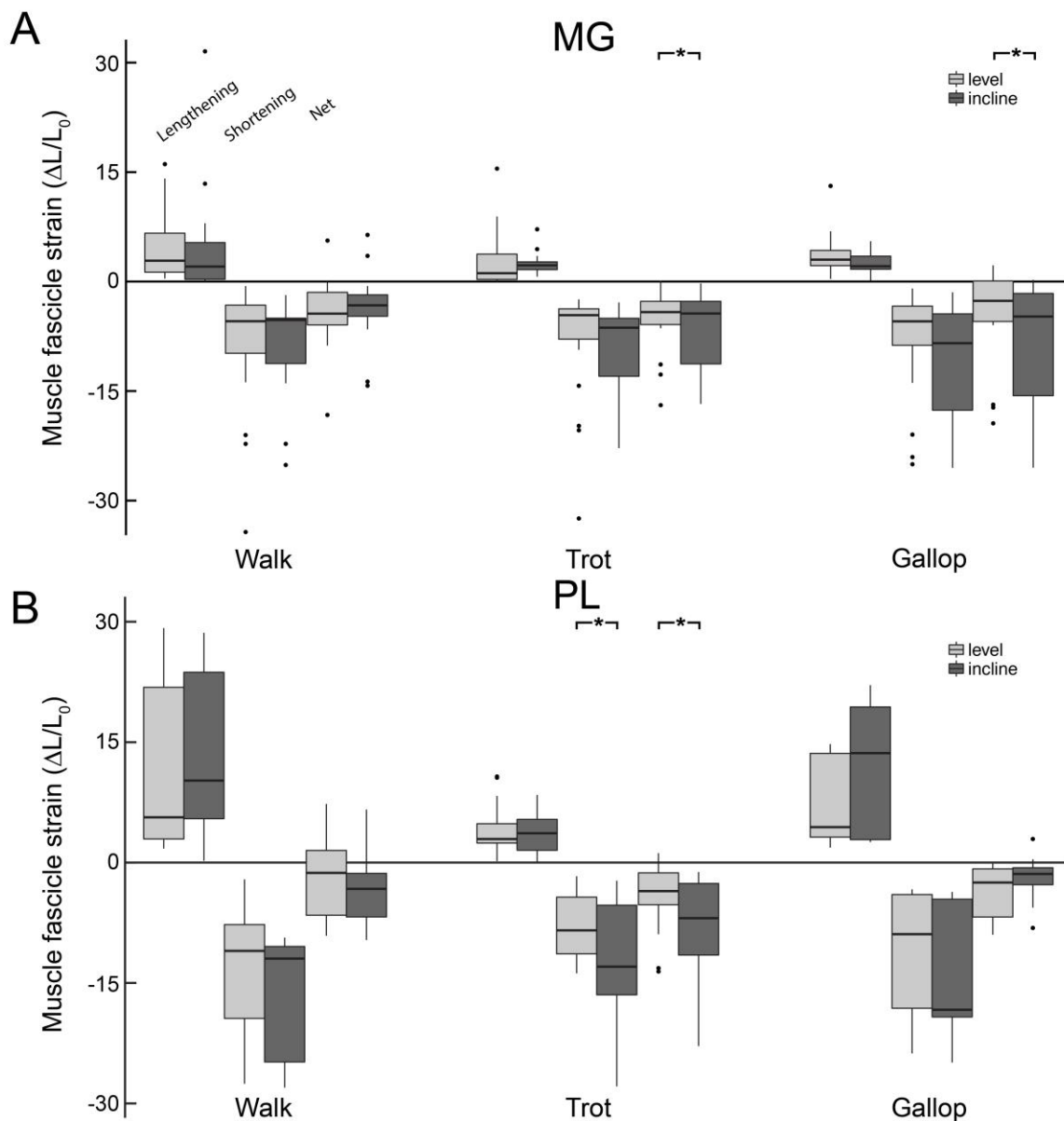


Figure 5. Boxplots showing average active lengthening, shortening, and net fascicle strain during force production in MG (A) and PL (B) for walk, trot, and gallop on level (light gray) and incline (dark gray) demonstrate that muscle fascicles undergo a combination of active lengthening and shortening during force production. Generally, similar patterns of fascicle strain are observed in the two muscles. Data reported as median with the bars extending to the first and third quartiles and whiskers showing the minimum and maximum values excluding outliers (greater than $1.5 \times \text{IQR}$), which are shown as single data points. Statistically significant differences are indicated with an asterisk for level vs. incline ($p < 0.05$) as evaluated using a general linear mixed model. $N=7$ for MG level walk, MG level trot; $N=6$ for MG incline trot, PL level walk, PL level trot; $N=5$ for MG incline walk, MG level gallop, PL incline trot; $N=4$ for MG incline gallop; $N=3$ for PL level gallop, PL incline gallop; and $N=2$ for PL incline walk.

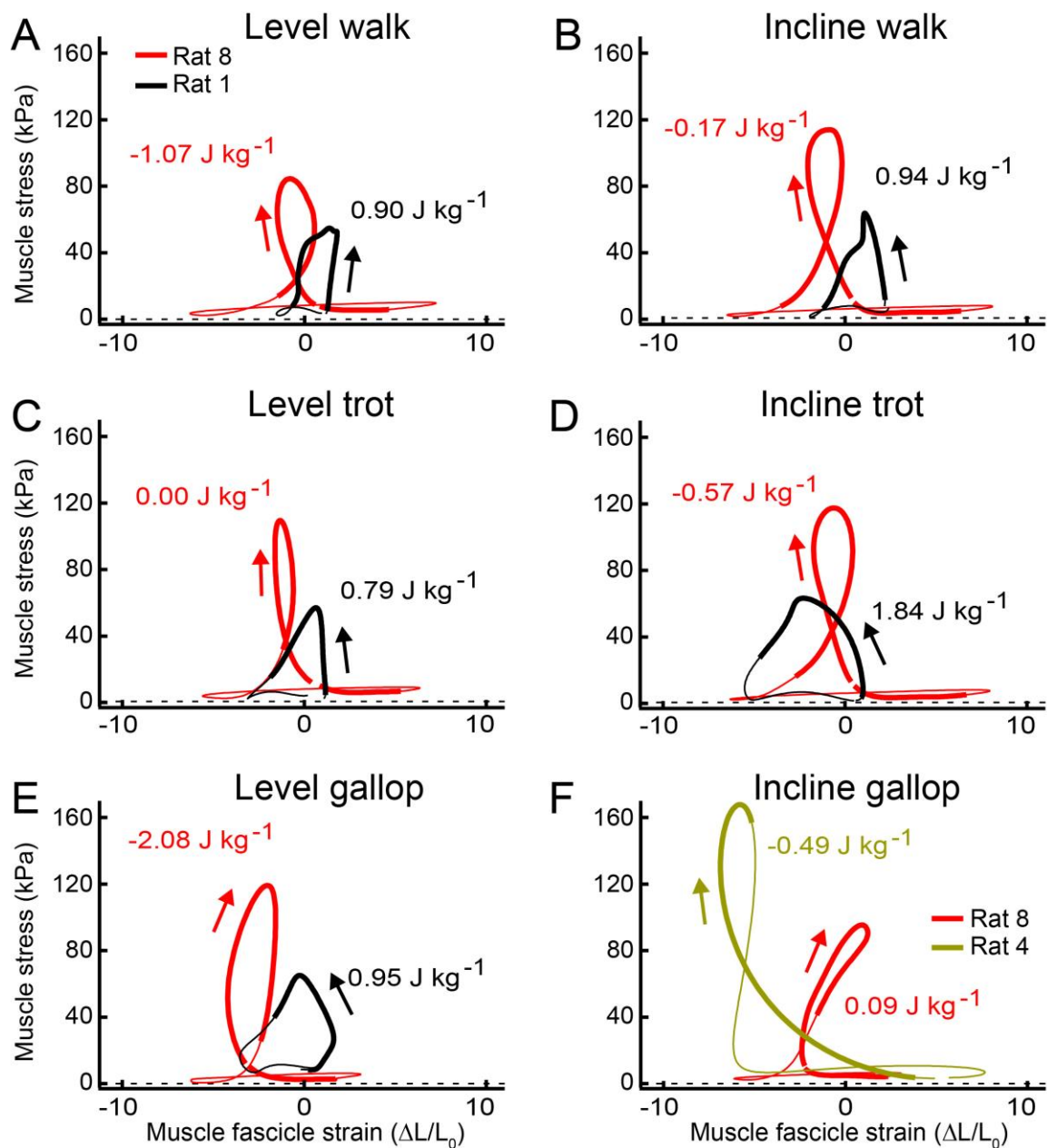


Figure 6. Mass-specific work loops of the MG plotted as muscle stress versus fascicle strain, for comparison between individuals (rat 1 & 8; note: a third rat 4 is shown for incline gallop, as these recordings were not obtained from rat 1). The direction of muscle stress relative to strain over the course of a complete stride cycle is shown by the arrows, together with the net mass-specific work ($J kg^{-1}$) performed by the muscle for each condition. Muscle activation (EMG) timing is indicated by the bold portion of each loop. Although variation in work loop patterns is observed between rats, across gait and grade conditions, the MG generally generates force with fascicle strains of $<6\%$: for rat 8 MG fascicle strains are $<4\%$, indicating largely isometric contractile behavior, whereas the MG of rat 1 (& rat 4, incline gallop) exhibits fascicle shortening early in force development. Net mass-specific muscle work is negative or low across all conditions.

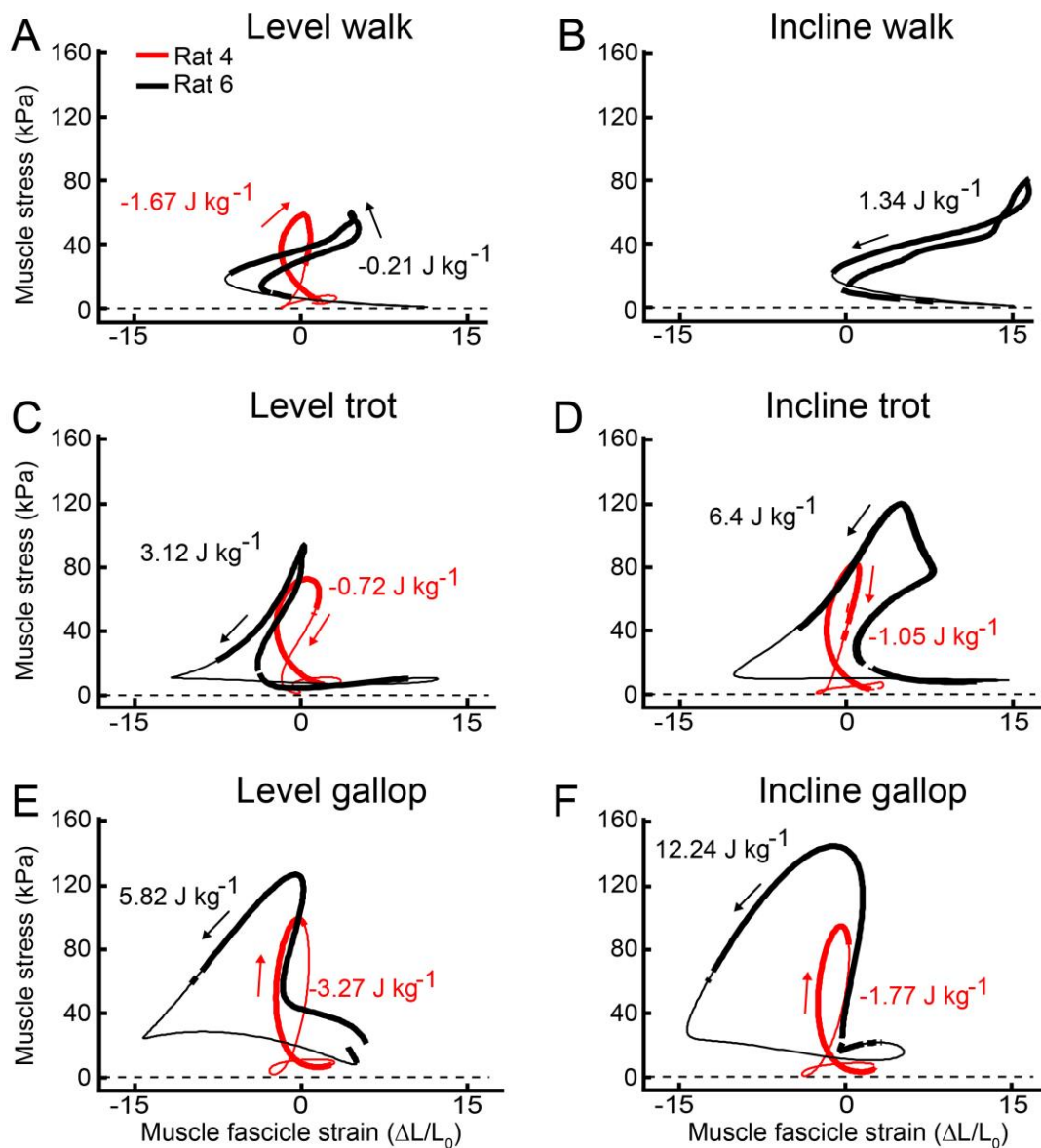


Figure 7. Mass-specific work loops of the PL plotted as muscle stress versus fascicle strain, for comparison between individuals (rat 4 & 6; although incline walk recordings were only obtained from rat 6). Net mass-specific work ($J\ kg^{-1}$) patterns are shown, as for the MG in Figure 7. Although variation in work loop patterns is observed between rats, across gait and grade conditions, the PL generally generates force with fascicle strains of $<15\%$: for rat 4 PL fascicle strains are $<3\%$, indicating limited length change behavior across all conditions, whereas rat 4 PL exhibits fascicle stretch followed by shortening during walking and trotting conditions, with increased net mass-specific work produced during incline versus level gait. Net mass-specific muscle work of rat 4 PL is negative and low across all conditions, with no evidence of increased net-positive work on an incline. Net mass-specific muscle work is greater in rat 6, with more evidence of increased net work on an incline for trotting and galloping.

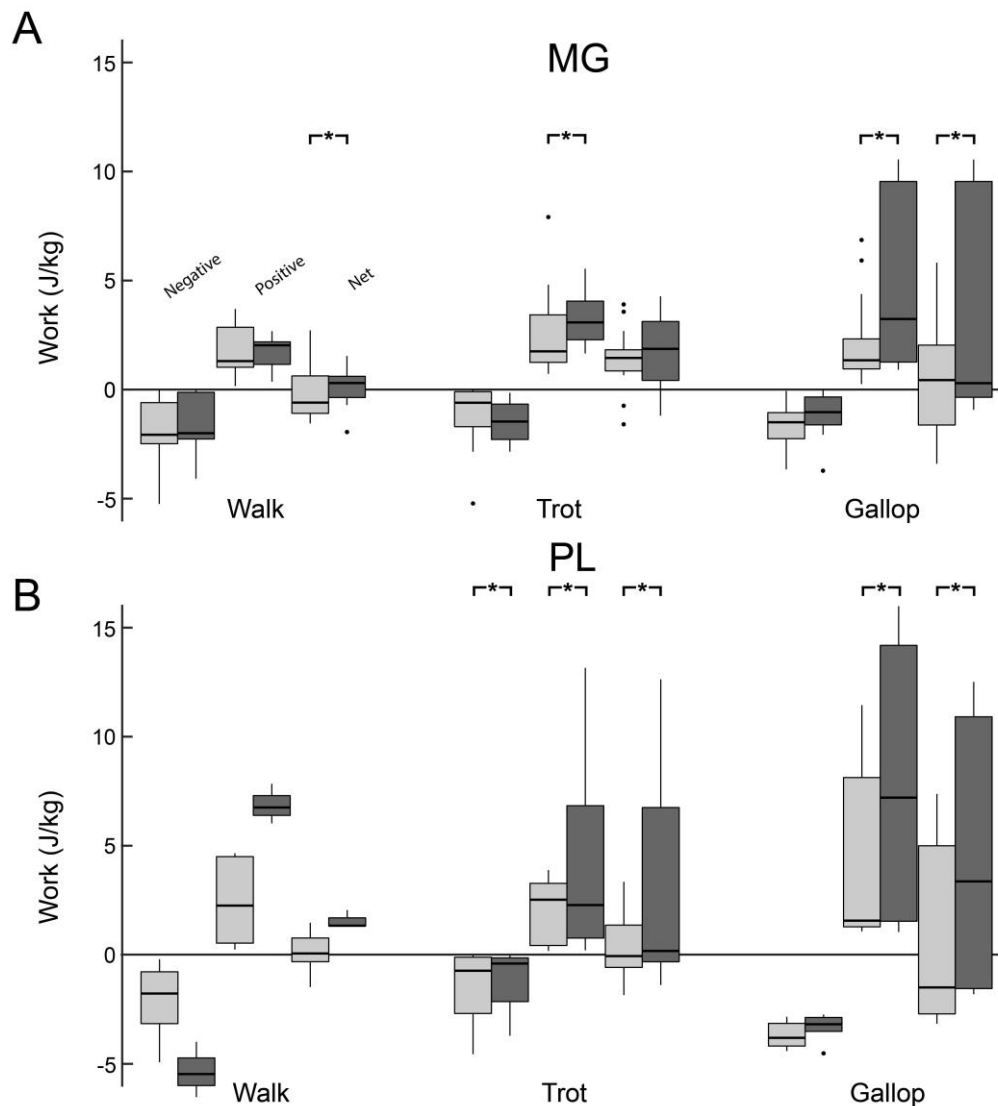


Figure 8. Box plots showing mass-specific negative, positive, and net muscle work performed during force production for walk, trot and gallop in the MG (A) and PL (B) on level (light gray) and incline (dark gray). The generally modest net fascicle strains observed in the two muscles (Fig. 5) result in generally low values of net muscle work. Net work was significantly greater on the incline compared with level for MG during walking and galloping and for PL during trotting and galloping. PL net work is greater for incline compared with level walking, but this difference cannot be statistically evaluated given $N=1$ for incline walk. Data reported as median with the bars extending to the first and third quartiles and whiskers showing the minimum and maximum values excluding outliers (greater than $1.5 \times IQR$), which are shown as single data points. Statistically significant differences are indicated with an asterisk ($p < 0.05$) as evaluated using a general linear mixed model. $N=6$ for MG level walk, MG level trot; $N=5$ for MG incline trot, PL level walk, PL level trot; $N=4$ for MG incline walk, MG level gallop, PL incline trot; $N=3$ for MG incline gallop; $N=2$ for PL level gallop, PL incline gallop; and $N=1$ for PL incline walk.

Tables

Table 1. P-values obtained using a general linear mixed model for the effect of gait and grade across rats

	Gait	Grade	Effect of gait			Effect of grade		
			Walk-Trot	Walk-Gallop	Trot-Gallop	Walk	Trot	Gallop
MG EMG intensity	<0.01	<0.01	0.21	<0.01	0.04	0.36	0.01	0.02
PL EMG intensity	0.01	0.03	0.46	0.01	0.05	0.01	0.28	0.04
MG peak stress	0.09	0.01	0.10	0.18	0.97	0.04	0.08	0.39
PL peak stress	0.02	0.37	0.10	0.01	0.24	0.99	0.40	0.75
MG net strain	0.51	0.04	0.61	0.51	0.95	0.68	0.02	<0.01
MG shortening strain	0.98	0.07	1.00	1.00	1.00	0.64	0.19	0.15
MG lengthening strain	0.43	0.64	0.48	0.52	1.00	0.48	0.59	0.14
PL net strain	0.33	<0.01	0.52	1.00	0.65	0.08	<0.01	0.29
PL shortening strain	0.32	0.02	0.22	0.87	0.54	0.87	<0.01	0.22
PL lengthening strain	0.16	0.95	0.17	0.98	0.33	0.22	0.84	0.08
MG net work	0.22	<0.01	0.28	0.28	0.98	0.05	0.13	0.01
MG positive work	0.17	<0.01	0.24	0.20	0.92	0.67	0.03	<0.01
MG negative work	0.43	0.43	0.47	0.50	0.99	0.11	0.26	0.32
PL net work	0.26	<0.01	NA	NA	0.59	NA	0.01	0.02
PL positive work	0.15	<0.01	NA	NA	0.22	NA	0.02	0.04
PL negative work	0.29	0.80	NA	NA	0.24	NA	0.04	0.37

Bolded values indicate p-value < 0.05.

Table 2. Average active distal limb muscle fascicle strains and mass-specific work compared across species for running and trotting.

Study	Muscle*	Condition	Lengthening strain (%)	Shortening strain (%)	Net strain (%)	Positive work (J kg ⁻¹)	Negative work (J kg ⁻¹)	Net work (J kg ⁻¹)
Daley and Biewener (2003) Guinea fowl	LG	Level run (1.3 m s ⁻¹)	2.0	-14.9	-12.9			7.7
	Dflex		13.0	-14.1	-1.1			-0.8
	LG	Incline run (16°, 1.3 m s ⁻¹)	2.0	-22.4	-20.4			12.0
	Dflex		8.0	-17.7	-9.7			5.3
Gabaldon et al. (2004) Turkey	LG	Level run (2.0 m s ⁻¹)			-5.0			2.0
	Per. long.				-12.0			4.7
	LG	Incline run (12°, 2.0 m s ⁻¹)			-12.0			7.0
	Per. long.				-19.0			8.1
Biewener et al. (1998) Wallaby	LG	Level hop (4.5 m s ⁻¹)	2.2	-1.2	1.0	4.3	-9.4	-5.0
	PL		2.1	-2.1	0.0	2.0	-2.8	-0.8
	LG	Incline hop (10°, 4.2 m s ⁻¹)	3.2	-2.4	0.8			-2.2
	PL		8.0	-7.6	0.4			-1.8
McGuigan et al. (2009) Goat	LG	Level trot (2.5 m s ⁻¹)	0.5	-16.4	-15.9			2.1
	MG		2.6	-11.3	-8.7			1.3
	SDF		4.2	-9.6	-5.4			0.5
	LG	Incline trot (15°, 2.5 m s ⁻¹)	0.4	-29.7	-29.3			8.3
	MG		0.0	-23.4	-23.4			7.5
	SDF		2.4	-10.3	-7.9			3.2
Eng et al. (this study) Rat	MG	Level trot (0.5 m s ⁻¹)	2.9	-7.8	-4.9	2.5	-1.1	1.4
	PL		3.9	-8.0	-4.1	2.0	-1.5	0.5
	MG	Incline trot (14°, 0.5 m s ⁻¹)	2.6	-9.2	-6.6	3.3	-1.5	1.8
	PL		3.9	-12.0	-8.2	4.2	-1.2	3.0

*LG: Lateral gastrocnemius; Dflex: Digital flexor; Per. long.: Peroneus longus; MG: Medial gastrocnemius; SDF: Superficial digital flexor; PL: Plantaris.

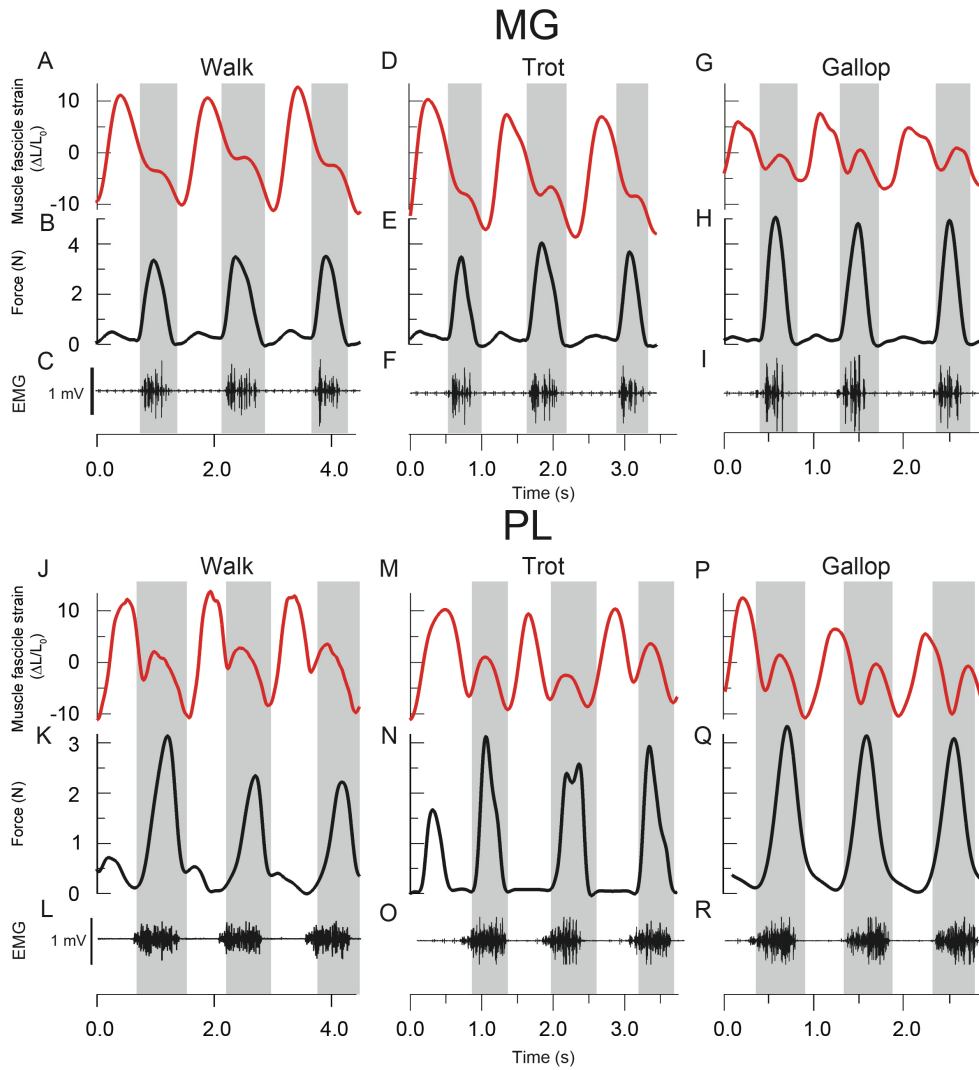


Figure S1. MG muscle fascicle strain (A, D, G), muscle force (B, E, H), and unamplified EMG (C, F, I) for level walk, trot, and gallop. PL muscle fascicle strain (J, M, P), muscle force (K, N, O), and unamplified EMG (L, O, R) for level walk, trot, and gallop. Gray regions represent the stance phase of each stride.

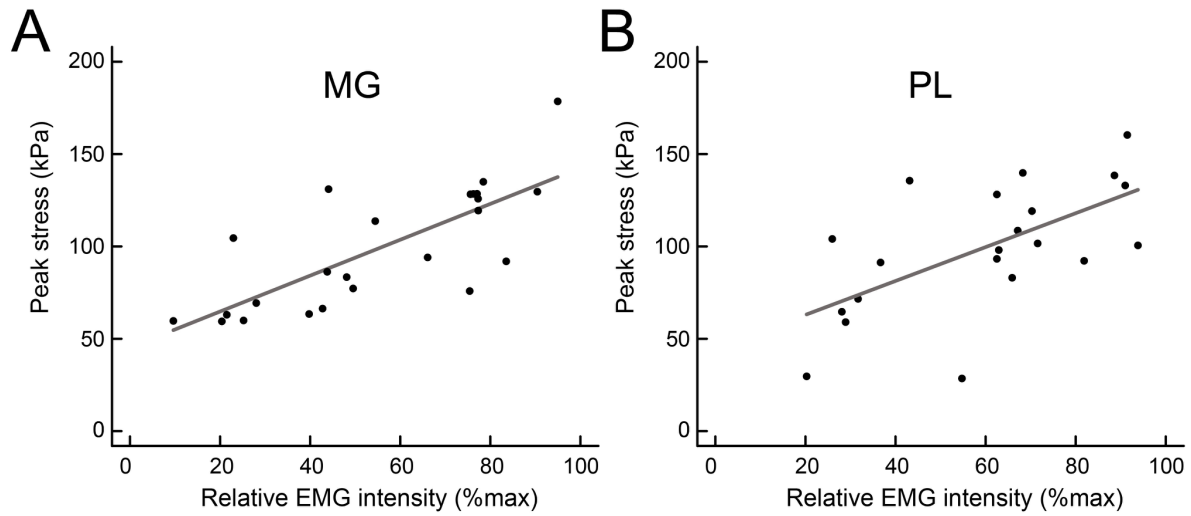


Figure S2. Peak stress (kPa) as a function of relative EMG intensity for the MG (A) and PL (B). The relationship between peak stress and relative EMG intensity evaluated with linear regression is significant for both MG ($p < 0.01$ and $R^2 = 0.58$) and PL ($p < 0.01$ and $R^2 = 0.38$).

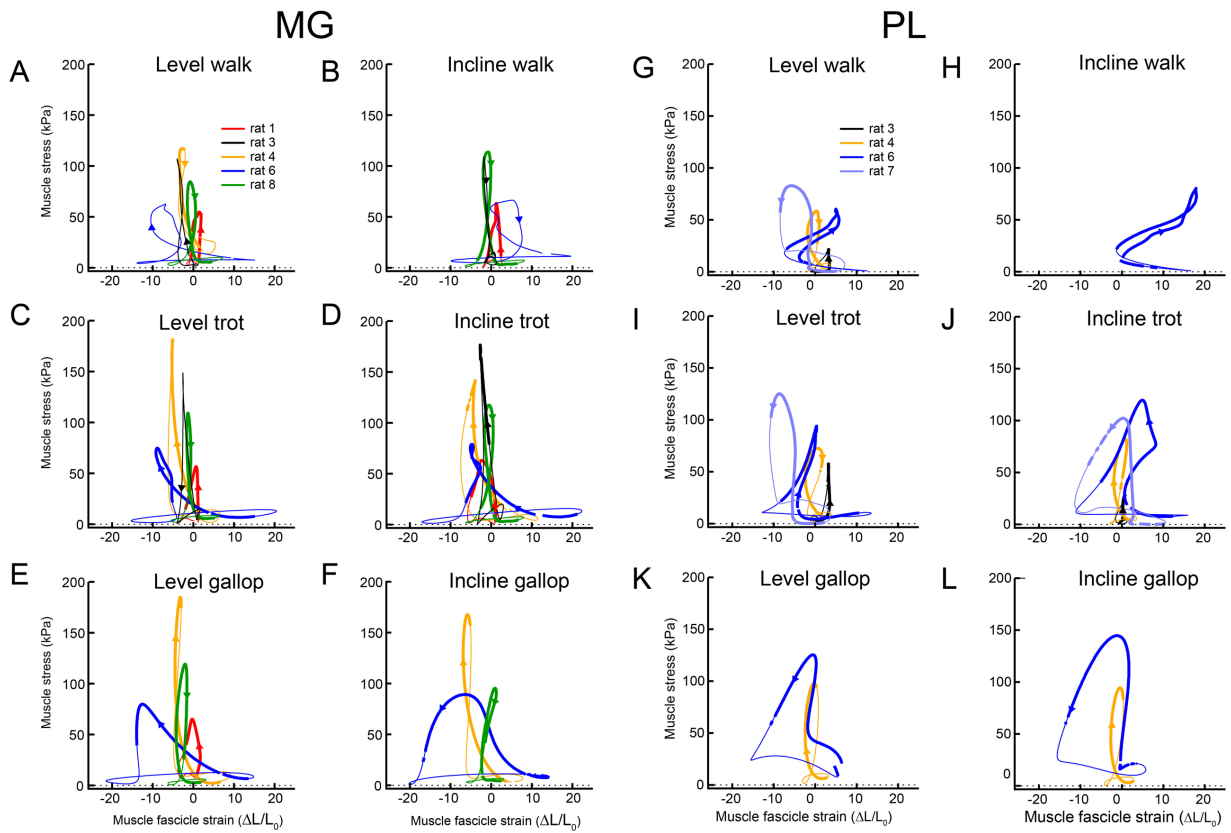


Figure S3. Mass-specific work loops of the MG (A-F) and PL (G-L) plotted as muscle stress versus fascicle strain, for comparison among multiple individuals. The direction of muscle stress relative to strain over the course of a complete stride cycle is shown by the arrows, together with the net mass-specific work (J kg^{-1}) performed by the muscle for each condition. Muscle activation (EMG) timing is indicated by the bold portion of each loop.

Table S1. Muscle architecture of medial gastrocnemius (MG) and plantaris (PL)

Muscle	Muscle mass (g)	Muscle length (mm)	Fascicle length (mm)	Pennation angle (degrees)	PCSA (mm ²)
MG	0.87 ± 0.08	31.13 ± 1.06	11.00 ± 0.93	26.4 ± 3.3	63.35 ± 14.39
PL	0.36 ± 0.03	35.15 ± 2.24	10.12 ± 0.21	18.4 ± 5.1	30.14 ± 3.66

Data are presented as mean ± s.e.m.

Table S2. Coefficients of variation across strides within an individual (individual) and across individuals (group) for level walk, trot, and gallop

	Walk		Trot		Gallop	
	Individual	Group	Individual	Group	Individual	Group
MG EMG intensity	17.0%	59.1%	20.0%	49.3%	19.2%	23.2%
PL EMG intensity	23.8%	63.1%	11.2%	52.9%	8.0%	13.4%
MG peak stress	6.9%	28.3%	6.7%	32.2%	12.1%	34.8%
PL peak stress	8.0%	38.3%	5.4%	28.1%	6.6%	2.8%
MG net strain	90.2%	83.1%	48.3%	71.5%	121.7%	145.0%
PL net strain	795.3%	531.1%	116.7%	100.0%	78.5%	76.6%
MG net work	56.0%	889.9%	4352.1%	69.7%	73.4%	281.0%
PL net work	187.3%	868.6%	31.9%	2320.1%	27.5%	355.3%

Table S3. P-values for non-parametric tests for the effect of gait and grade across rats

	Effect of gait: Level			Effect of gait: Incline			Effect of grade		
	Walk-Trot	Walk-Gallop	Trot-Gallop	Walk-Trot	Walk-Gallop	Trot-Gallop	Walk	Trot	Gallop
MG EMG intensity	0.16	0.03	0.06	0.06	0.13	0.13	0.31	0.16	0.06
PL EMG intensity	0.28	0.13	0.13	0.06	0.06	0.06	0.78	0.50	0.88
MG peak stress	0.02	0.06	0.13	0.06	0.13	0.56	0.44	0.38	0.22
PL peak stress	0.06	0.25	0.25	0.25	0.25	0.19	0.75	0.50	0.81
MG net strain	0.96	0.69	0.41	0.78	0.63	0.69	0.78	0.97	1.00
MG shortening strain	0.15	0.78	0.91	0.69	0.63	0.69	0.69	0.84	1.00
MG lengthening strain	0.96	0.78	0.31	0.59	1.00	0.69	0.50	0.28	0.88
PL net strain	0.89	0.88	0.38	1.00	0.50	0.13	1.00	0.94	0.25
PL shortening strain	0.11	0.38	0.75	0.50	0.75	0.63	0.50	0.91	0.75
PL lengthening strain	0.89	0.88	0.63	0.75	0.50	0.25	0.75	0.78	0.25
MG net work	0.02	0.31	0.69	0.13	0.25	0.38	0.06	0.06	0.25
MG positive work	0.02	0.19	0.31	0.13	0.50	0.63	0.56	0.06	0.13
MG negative work	0.02	0.56	0.69	0.69	0.25	0.63	0.19	0.78	0.25
PL net work	0.78	0.50	0.50	NA	NA	0.50	NA	0.13	0.25
PL positive work	0.78	0.25	0.50	NA	NA	0.50	NA	0.31	0.25
PL negative work	0.69	0.75	0.75	NA	NA	1.00	NA	0.13	0.50

Bolded values indicate p-value < 0.05